Performance analysis of two tier HetNets with massive MIMO enabled wireless backhauling

Article *in* Wireless Networks · December 2019

DOI: 10.1007/s11276-019-02205-1

3 authors, including:

Shweta Rajoria

5 PUBLICATIONS **12** CITATIONS

SEE PROFILE

Aditya Trivedi

ABV-Indian Institute of Information Technology and Management Gwalior

125 PUBLICATIONS **263** CITATIONS

SEE PROFILE

Performance analysis of two tier HetNets with massive MIMO enabled wireless backhauling

Shweta Rajoria, Aditya Trivedi & W. Wilfred Godfrey

Wireless Networks
The Journal of Mobile Communication, Computation and Information

ISSN 1022-0038
Volume 26
Number 2

Wireless Netw (2020) 26:1459-1472
DOI 10.1007/s11276-019-02205-1

Springer

Wireless Networks (2020) 26:1459–1472
https://doi.org/10.1007/s11276-019-02205-1

Performance analysis of two tier HetNets with massive MIMO enabled wireless backhauling

Shweta Rajoria[1] · Aditya Trivedi[1] · W. Wilfred Godfrey[1]

Published online: 12 December 2019

Abstract
Dense deployment of small cells escalates the network capacity, making it a candidate technology for the future wireless network. However, backhauling of such a large number of small cells becomes a major challenge in its successful deployment. In this paper, a framework for massive MIMO enabled wireless backhauling in a two-tier heterogeneous network is developed. The framework considers massive MIMO enabled macro base station and in-band full-duplex (IBFD) small cell base station. Massive MIMO system provides high spectral efficiency and high energy efficiency. Besides, due to IBFD capability, the small cells can utilize the same frequency band to communicate over the access link and the backhaul link simultaneously. Tools from the stochastic geometry are utilized to model and derive the analytical expressions of coverage probability and area spectral efficiency (ASE). Furthermore, a trade-off between ASE and coverage probability is observed. All the analytical results are verified by simulation. Simulation results show that massive MIMO and IBFD communication may be useful technologies from the backhauling perspective in the dense small cell network. It is observed that the proposed framework provides 42.30% improvement in the coverage performance over the other existing framework for rate threshold of 1 bps/Hz. Furthermore, optimal performance for the proposed model can be achieved by tuning of bandwidth allocation factor.

Keywords Backhauling · Heterogeneous networks · Massive MIMO · Small cell · Stochastic geometry

1 Introduction

The ever escalating growth of mobile data traffic in recent past is a foreteller of prodigious sized traffic in future, brings out the need to increase the capacity of wireless network. According to Cisco Visual Networking Index (VNI) forecast, global mobile data traffic will increase seven fold from 2017 to 2022 [1]. This necessitates next generation (5G) to introduce new technologies that aims at high data rate, better coverage, and huge capacity in order to fulfil the demand. Dense heterogeneous network, typically macro base station (MBS) overlaid with large number of small cell base stations (SBSs) is identified as a key solution to achieve high throughput, coverage, and energy efficiency (EE) [2–4]. However, employing wired backhaul connectivity to large number of small cells is a major bottleneck to do in practice. Wireless backhauling through massive MIMO may be an imperative and cost efficient solution [5–7]. Massive MIMO is a technique in which hundreds of antennas are used at the base station to serve multiple users simultaneously at the same time and frequency resource block [8]. Besides this, massive MIMO enhances spectral efficiency (SE) and EE of wireless cellular network and is going to be considered as an essential element of future network [8, 9]. Furthermore, recent advancements in self interference (SI) cancellation ability of full-duplex radios through shared antenna scheme, digital circuit domain scheme, beamforming based techniques, etc., sparkles the way of its successful deployment [10–12]. In-band full-duplex (IBFD) systems enable transmission and reception of information in same frequency band and

✉ Shweta Rajoria
shwtrajoria@gmail.com; shweta@iiitm.ac.in

Aditya Trivedi
atrivedi@iiitm.ac.in

W. Wilfred Godfrey
godfrey@iiitm.ac.in

[1] ABV-Indian Institute of Information Technology and Management, Gwalior 474015, India

achieve remarkable improvement in SE of a wireless network [13]. Hence, the use of full-duplex technique at SBS and massive MIMO at MBS for in-band backhaul transmission imparts an excellent architecture [6, 13, 14] merging the benefits of foregoing techniques.

1.1 Related work and motivation

Aforementioned literature emphasizes the benefits of heterogeneous networks, full-duplex techniques, and massive MIMO systems. Henceforth, this section discusses potential work enhancement brought by the existing literature in the subsequent technologies. Authors in [15] have developed a K tier heterogeneous network model using stochastic geometry tools and have also derived the closed form expressions of coverage probability and outage probability. The paper has manifested that the proposed network model is as good as an actual 4G macro-cell deployment model. In [16], an expression for EE is provided for two-tier heterogeneous network with multiple antennas both at the MBS and SBS. In particular, joint bandwidth allocation and power allocation scheme is presented to optimize the obtained EE. Literature provided in [5, 17–19] has laid solid foundation for Massive MIMO in heterogeneous network. In [18], authors have derived the expressions of rate and coverage and has also examined the impact of massive MIMO on user association in K tier heterogeneous cellular network. Results have shown considerable improvement in the performance of heterogeneous cellular network with the use of massive MIMO. The expressions of outage probability and transmission rate are derived in [17] for K tier heterogeneous network by employing massive MIMO, mm-wave, and beamforming techniques. SE and EE analysis of massive MIMO enabled K tier heterogeneous network is discussed in [19]. Authors have examined flexible cell association, load balancing conditions and have also proved that a moderate amount of user off-loading can improve both SE and EE. Trade-off between success probability and area spectral efficiency (ASE) for multi user MIMO heterogeneous network is provided in [20]. Furthermore, an optimization problem is designed to find the optimal value of base station density which results in maximizing ASE and satisfies a given link requirement for reliable communication. In [21], data transmission approaches are proposed for multiuser massive MIMO systems while considering the spatial basis expansion channel model and user scheduling for data transmission. In [22], a sparse Bayesian learning framework based channel estimation strategy is proposed for multi-cell massive MIMO systems. The proposed estimation strategy can be applied for both up-link and down-link channel estimation in time division duplex and frequency division duplex systems. Furthermore, a two-stage precoding scheme based on interference alignment and soft-space-reuse is proposed for multi-cell scenario in massive MIMO systems to improve the capacity of cell edge users in [23]. The rate coverage and ASE analysis for massive multi-user MIMO system with full-duplex small cell are provided in [24]. From the results, it is observed that equipping massive MIMO at MBS improves downlink coverage probability whereas, ASE improves with the increase in full-duplex SBSs.

However, the aforestated articles do not consider the concept of backhauling. In [25], in-band full-duplex backhauling in two-tier heterogeneous network is studied. For the clear explanation of the concept of frequency division duplexing, authors have considered the same analysis as employed for time division duplexing with the change of replacing frequency by time slot. Theoretical framework for Massive MIMO backhauling in heterogeneous network and its potential benefits are provided in [5, 26]. In [5], massive MIMO provides wireless backhauling in ultra-dense network and renders remarkable improvement in throughput. Theirin, it is shown that in-band backhaulig through massive MIMO is a feasible solution and is less costlier than mm-wave or wired backhaulig. While in [26] from the perspective of backhauling, a brief idea of beamforming, uplink downlink capacity, and channel estimation is provided. Energy efficiency analysis of MIMO backhaul network for uplink and down link transmission is discussed in [7]. Results reveal that EE of heterogeneous network is highly sensitive to network load irrespective of the deployment strategy, under spatial multiplexing consideration. Hence, bandwidth allocation between access link and backhaul link must be optimally designed. Power optimization problem for a full-duplex self-backhaul heterogeneous network with massive MIMO is discussed in [12]. Backhaul delay minimization policy is discussed in [27], and in particular Chen et.al., also derive total expected delay accounting retransmission of information in the network.

Massive MIMO backhauling with IBFD techniques is less studied in the available literature, where as contribution of papers [25, 28] are the attempts in this direction. Energy efficiency analysis for the IBFD massive MIMO network is presented in [28] and spectral efficiency analysis for the same is performed in [29, 30]. In [28], precoding scheme is designed to reduce interference and later on optimization problem is formulated by implying sleep mechanism for the SBS. In [29], user association and resource allocation optimization problem is formulated to maximize SE of the proposed system model. Furthermore, work closely related to the proposed idea is presented in [6]. Authors have investigated massive MIMO enabled MBS which contributes wireless backhauling in two-tier network. However, in the paper, MBS only provides

backhaul connections to the small cells and does not participate in access communication to users. MBS is working as a connector node. The work mainly focuses on exhibiting the significance of in-band and out-band full-duplex communication to achieve satisfactory performance. Different from [6], MBS in the proposed work allows transmission for access link (MBS to user) and backhaul link (MBS to SBS) simultaneously. Bandwidth partitioning is employed to achieve the same. η part of the whole bandwidth is allotted for access link (MBS to user) and $(1-\eta)$ for the backhaul link (MBS to SBS). Furthermore, we analyze the ASE for the proposed model and discuss trade-off between ASE and coverage probability. Numerical results impart some insight into the impact of different parameters on the trade-off to show the practicability of the proposed architecture in the real time. Numerical results have also shown improvement in the performance of the proposed model over [6] with the integration of access link from MBS.

Our major contributions are as follows.

- Tools from the stochastic geometry are used to design a two-tier heterogeneous network with massive MIMO. Tier 1 consists of macro BS with massive MIMO provides backhaul link and access link transmissions, and operates in half duplexed mode. Whereas second tier consists of SBSs which operate in in-band full-duplex mode to achieve high ASE.
- For the proposed system model, interferences for various links are characterized. Analytical expressions of coverage probability and ASE are derived for downlink transmission by applying stochastic geometry and Gil-Pelaez theorem. Numerical results are verified by simulation and compared with the results of those mentioned in [6]. The results presented in the paper demonstrate the effect of BS density, number of antennas, path-loss exponent, and BS powers on the performance of network.
- Trade-off between ASE and coverage probability is discussed to manifest the practical deployment of the proposed work in real time. It is observed that bandwidth allocation factor plays vital role in performance measures.

The remainder of this paper is structured as follows. Section 2 discusses the system model of the proposed two-tier heterogeneous network. It describes network model, channel model, backhaul model, and association model. Interference characterization, SINR model, and rate model formulation are provided in Sect. 3. In Sect. 4, coverage probability expressions for access link and backhaul link are derived. Then ASE expression for the proposed MIMO heterogeneous network is presented. Section 5 illustrates the numerical results and lastly, the paper is concluded in Sect. 6.

2 System model

System model considered in this paper is detailed in the following sub-sections.

2.1 Network model

Consider a downlink two-tier heterogeneous network comprises of MBS with massive antennas and SBS with single antenna as shown in Fig. 1. MBS imparts backhaul data transmission for all the SBSs in its range wirelessly. All the MBSs and SBSs are spatially placed in $\mathbb{R}^2$ and assume to follow the independent homogeneous Poisson point process (PPP) ϕ'_x and ϕ'_y with density λ'_m and λ'_s, respectively. Transmission powers for MBS and SBS are considered as P_m and P_s, respectively. MBS operates in conventional half duplex mode and SBS operates in in-band full-duplex mode, i.e., it can transmit and receive at the same time and frequency resource block. Withal, a time division duplexing scheme is considered with perfect channel state information (CSI) to facilitate channel estimation by exploiting the property of channel reciprocity. Users positioning is also designed with independent PPP ϕ'_u with density λ'_u. Analysis performed throughout the paper considers a user with single antenna and is placed at the origin. The analysis at the origin is possible by virtue of Slivnyak's theorem [31]. According to the theorem, properties beheld by a user located anywhere in ϕ'_u are same as those beheld by the user at origin in the point process ϕ'_u.

2.2 Channel model

In the proposed channel model, link incorporates small scale fading, large scale fading, and path loss. Channel between any two nodes is assumed to be independent and identically distributed. Path loss between any two nodes is given as $X_{AB}^{-\delta}$, where X_{AB} is the distance between node A and B and δ is the path loss exponent. Small scale fading is modeled by Rayleigh distribution in the proposed model. Large scale fading is modeled as log normal distribution with mean μ_{AB} and standard deviation of channel power σ_{AB}, respectively. Similar to [6], displacement theorem is applied to incorporate the effect of shadow fading S_{AB}.

$$E\left[S_{AB}^{2/\delta}\right] = \exp\left(2\frac{\mu_{AB}}{\delta} + 0.5\left(2\frac{\sigma_{AB}}{\delta}\right)^2\right), \quad (1)$$

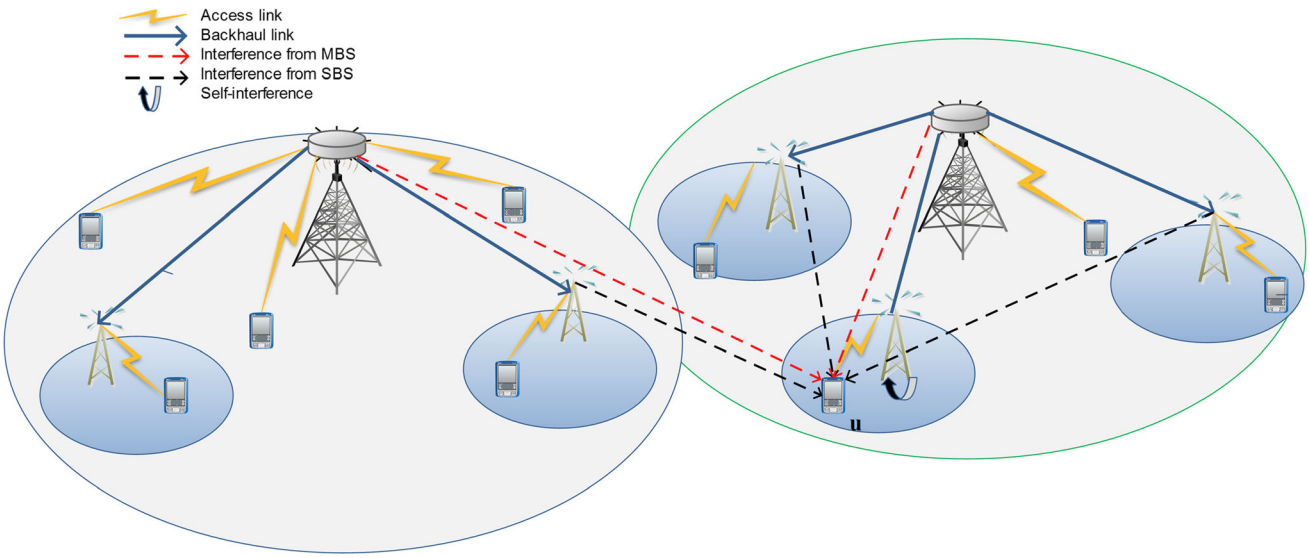

Fig. 1 Example of proposed massive MIMO enabled two-tier heterogeneous network depicting wireless backhauling and in-band full-duplex communication. For the ease of exposition all the interference links are illustrated at *u th* user only

Hence, new densities become $\lambda_m = \lambda'_m E\left[S_{AB}^{2/\delta}\right]$ and $\lambda_s = \lambda'_s E\left[S_{AB}^{2/\delta}\right]$. Correspondingly, ϕ'_x and ϕ'_y become ϕ_x and ϕ_y, respectively.

2.3 Massive MIMO backhaul model

MBS is retaining N number of antennas and is supporting L numbers of downlink data streams. Whereas, K be the total number of SBSs and for the massive MIMO $K \leq L \leq N$ [8, 32]. MBS is using linear Zero Forcing Beamforming (ZFBF) technique to lay out downlink transmission with equivalent power distribution per link. In the course of training phase, MBS receives pre-assigned orthogonal pilot sequences from both SBSs and users, and then it estimates them perfectly without any pilot contamination.[1] Due to deployment of massive MIMO at MBS and applying ZFBF in that, interference among the multiple backhaul links can be mitigated. This makes it more beneficial for in-band transmission. As the channel hardening effect in massive MIMO systems results in averaging out of small scaling fading [33], the paper considers large scale fading and path loss.

2.4 Association model

Cell association follows the maximum average received power approach as detailed in [34] that allows a user to connect with SBS even if the power received from MBS is higher. This helps to reduce load at MBS by off-loading traffic from MBS. If T_m and T_s represent the distance of a user from the closest BS in ϕ_x and ϕ_y, respectively then from [34], average received power of MBS and SBS can be defined as follows

$$P_m{}' = \frac{N-L-1}{L} P_m |T_m|^{-\delta}, \tag{2}$$

$$P_s{}' = P_s |T_s|^{-\delta}. \tag{3}$$

Considering the aforementioned association rule, association probabilities of MBS and SBS are derived in the following Lemmas.

Lemma 1 *Probability that user associated with MBS is derived as*

$$\Pi_m = 2\pi\lambda_m \times \int_0^\infty t \exp\{-\pi\lambda_m t^2 - \pi\lambda_s \left(\frac{LP_s}{(N-L-1)P_m}\right)^{2/\delta} t^2\} dt. \tag{4}$$

Proof The expression in (4) is derived by slight modifications in Lemma 1 of [34] and proof for the same is given in "Appendix 1". □

Lemma 2 *Probability of user association with SBS is derived as*

[1] Assumption for no pilot contamination is valid as numerous pilot contamination mitigation techniques have been developed in the existing literature [8, 9, 15].

$$\Pi_s = 2\pi\lambda_s \times \int_0^{\infty} t \exp\{-\pi\lambda_s t^2 - \pi\lambda_m \left(\frac{(N-L-1)P_m}{LP_s}\right)^{2/\delta} t^2\} dt. \quad (5)$$

Proof The proof can be obtained by following the similar procedure to Lemma 1.

Furthermore, probability density function (PDF) of distance between a typical user and its corresponding BS is evaluated from the results of [34]. Henceforth, the PDF of the distance between when a user is connected MBS is delineated as

$$f_{X_{m,u}}(x_{m,u}) = \frac{2\pi\lambda_m}{\Pi_m} x_{m,u} \times e^{\left[-\pi\lambda_m x_{m,u}^2 - \pi\lambda_s \left(\frac{LP_s}{(N-L-1)P_m} x_{m,u}^2\right)\right]}, \quad (6)$$

Similarly, the PDF of the distance between the typical user and its associated SBS is given as

$$f_{X_{s,u}}(x_{s,u}) = \frac{2\pi\lambda_s}{\Pi_s} x_{s,u} e^{\left[-\pi\lambda_s x_{s,u}^2 - \pi\lambda_m \left(\frac{(N-L-1)P_m}{LP_s} x_{s,u}^2\right)\right]}. \quad (7)$$

□

3 Performance metric and SINR model

In this section, rate equations and SINR equations for access links (between MBS and user and between SBS and user) and backhaul link (MBS to SBS) are formulated. Interference characterization from different source of interferences is also discussed which is necessary in the performance evaluation of proposed massive MIMO enabled heterogeneous network.

3.1 Rate equations

Normalized rate (in bits per second per Hz) is used in the entire analysis. As in-band backhaul transmission scheme is adopted, η portion of bandwidth is used for the access link from MBS to user and $(1-\eta)$ is used for both access link from SBS to user and backhaul link from MBS to SBS. Downlink rate for the access link from MBS to user link ($R_{a,m}$) is delineated as [30]

$$R_{a,m} = \eta \log_2\left(1 + \frac{N-L-1}{L} SINR_{a,m}\right), \quad (8)$$

where η is the bandwidth allocation factor, $(N-L-1)/L$ is the gain of ZFBF technique [30], and $SINR_{a,m}$ is the SINR of a user when served by MBS, which is explained later in Sect. 3.2. Downlink rate for the access link from SBS to user link ($R_{a,s}$) is

$$R_{a,s} = (1-\eta)\log_2\left(1 + SINR_{a,s}\right), \quad (9)$$

where $SINR_{a,s}$ is the signal to noise plus interference ratio of SBS to user link.

Similarly, rate of MBS to SBS backhaul link while accounting downlink transmission is provided as

$$R_b = (1-\eta)\log_2\left(1 + \frac{N-K-1}{K} SINR_b\right). \quad (10)$$

3.2 SINR model

1. *Access link from MBS to user:* SINR of a user located at the origin when connected with MBS is given as

$$SINR_{a,m} = \frac{P_m |X_{m,u}|^{-\delta}}{I_{m,u_m} + I_{s,u_m} + N_0}, \quad (11)$$

where X_{mu} is the distance between MBS and user. I_{m,u_m} and I_{s,u_m} are the interferences experienced by the user associated with MBS from other MBSs and SBSs, respectively and can be calculated as

$$I_{m,u_m} = \sum_{i \in \Phi_x/m} P_m |X_{i,u}|^{-\delta}, \quad (12)$$

$$I_{s,u_m} = \sum_{j \in \Phi_y} P_s g_{j,u} |X_{j,u}|^{-\delta}. \quad (13)$$

In (11), small scale fading term is not considered as, it averages out due to channel hardening effect which is an inherent property of massive MIMO and N_0 indicates the noise power. $g_{j,u}$ in the interference term (I_{s,u_m}) represents small scale fading gain between *jth* SBS and *uth* user.

2. *Access link from SBS to user:* SINR of a user located at the origin while associated with SBS is given as

$$SINR_{a,s} = \frac{P_s g_{s,u} |X_{s,u}|^{-\delta}}{I_{m,u_s} + I_{s,u_s} + N_0}, \quad (14)$$

where $X_{s,u}$ is the distance between SBS and user, and $g_{s,u}$ is the small scale fading experienced by the channel which is Rayleigh distributed as stated earlier. I_{s,u_s} and I_{m,u_s} are the interferences experienced by user from the other SBSs and MBSs, respectively and are modeled as

$$I_{s,u_s} = \sum_{j \in \Phi_y/s} P_s g_{j,u} |X_{j,u}|^{-\delta}, \quad (15)$$

$$I_{m,u_s} = \sum_{i \in \Phi_x} P_m |X_{i,u}|^{-\delta}. \quad (16)$$

3. *Backhaul link:* SINR of MBS to SBS backhaul link is given as

$$SINR_b = \frac{P_m |X_{m,s}|^{-\delta}}{I_{m,s} + I_{s,s} + \alpha P_s}, \tag{17}$$

where $X_{m,s}$ is the distance between MBS and SBS. $I_{m,s}$ and $I_{s,s}$ are the interferences experienced by SBS from the other MBSs and SBSs, respectively and are modeled as

$$I_{m,s} = \sum_{i \in \Phi_x / m} P_m |X_{i,s}|^{-\delta}, \tag{18}$$

$$I_{s,s} = \sum_{j \in \Phi_y / s} P_s \, g_{j,s} |X_{j,s}|^{-\delta}, \tag{19}$$

and αP_s denotes self residual interference of the full-duplex SBS and this interference is received at SBS from its own transmitting signal due to operating in IBFD mode [35]. Note that α is a self- interference controlling factor and is characterized according to the self-interference cancellation algorithm [36]. Though in this work, α is considered as a constant value to simplify the model.

4 Coverage probability and ASE

In this section, rate coverage probability and ASE for the proposed system model are derived.

4.1 Coverage probability

Coverage probability is defined as the probability of a randomly chosen user's SINR in given network should be greater than a particular SINR threshold. Besides, for the successful transmission each link must achieve minimum R_{th} rate. Herein, it is assumed that $\tau_{a,m}$, $\tau_{a,s}$, and τ_b be the SINR threshold of the following links: MBS to user, SBS to user, and MBS to SBS link, respectively and can be evaluated from (8), (9), and (10) by substituting R_{th}. In the proposed system model, coverage probability of a typical user is influenced by both MBS to user link and MBS to SBS to user link. Hence, overall coverage probability is given as

$$C = \Pi_m C_m + \Pi_s C_s, \tag{20}$$

where the values of Π_m and Π_s can be obtained from (4) and (5), respectively. Moreover, downlink coverage probability if a user is served by MBS is denoted as C_m and is given as

$$C_m = p\left[SINR_{a,m} > \tau_{a,m}\right]. \tag{21}$$

Herein $\tau_{a,m} = \frac{L}{N-L-1}\left(2^{\frac{R_{th}}{\eta}} - 1\right)$. Furthermore, C_s shows the coverage probability of a user served by SBS and is modeled as the product of coverage probability of backhaul link (MBS to SBS) and access link (SBS to user). Since both links are considered independent, it can be calculated as

$$C_s = p\left[SINR_{a,s} > \tau_{a,s}\right].p[SINR_b > \tau_b], \tag{22}$$

where $\tau_{a,s} = \left(2^{\frac{R_{th}}{(1-\eta)}} - 1\right)$ and $\tau_b = \frac{K}{N-K-1}\left(2^{\frac{R_{th}}{(1-\eta)}} - 1\right)$.

Theorem 1 *Downlink coverage probability when a user is connected with MBS is given as*

$$C_m = \frac{2\pi\lambda_m}{\Pi_m} \int_0^\infty x_{m,u} \left[\frac{1}{2} - \frac{1}{\pi} T_1(x)\right] \times e^{\left[-\pi\lambda_m x_{m,u}^2 - \pi\lambda_s \left(\frac{LP_s}{(N-L-1)P_m} x_{m,u}^2\right)\right]} dx_{m,u}, \tag{23}$$

where

$$T_1(x) = \int_0^\infty Im[\exp(\psi_1(x,\omega) + \psi_2(x,\omega) + \psi_3(x,\omega))] \frac{d\omega}{\omega}, \tag{24}$$

$$\psi_1(x,\omega) = -\pi\lambda_m \left(\frac{\left|1 - \frac{2}{\delta}\right| + \frac{2}{\delta}\left|\frac{-2}{\delta}, \frac{j\omega P_m}{x_{m,u}^\delta}\right|}{(j\omega P_m)^{-2/\delta}} - x_{m,u}^2 \right), \tag{25}$$

$$\psi_2(x,\omega) = \frac{2\pi\lambda_s}{\delta - 2} (j\omega P_s)^{2/\delta} \left|2 - \frac{2}{\delta}\right| \left|\frac{2}{\delta}\right|, \tag{26}$$

$$\psi_3(x,\omega) = -j\omega \left(\frac{P_m}{\tau_{a,m} x_{m,u}^\delta} - N_0 \right). \tag{27}$$

Proof See "Appendix 2". □

Theorem 2 *Downlink coverage probability when a user is connected with SBS is given as*

$$C_p = \frac{2\pi\lambda_s}{\Pi_s} \times \int_0^\infty x_{s,u} \exp[\varpi_1(x) + \varpi_2(x) + \varpi_3(x)\varpi_4(x)] dx_{s,u}, \tag{28}$$

where

$$\varpi_1(x) = -\pi\lambda_m x_{s,u}^2 \left(\frac{\tau_{a,s} P_m}{P_s}\right)^{2/\delta} \left|1 - \frac{2}{\delta}\right|, \tag{29}$$

$$\varpi_2(x) = -\frac{2\pi\lambda_s \tau_{a,s}}{\delta - 2} x_{s,u}^2 {}_2F_1\left[1, 1 - \frac{2}{\delta}, 2 - \frac{2}{\delta}, \tau_{a,s}\right], \tag{30}$$

$$\varpi_3(x) = -\frac{\tau_{a,s} x_{s,u}^\delta N_0}{P_s}, \tag{31}$$

$$\varpi_4(x) = -\pi\lambda_s x_{s,u}^2 - \pi\lambda_m\left(\frac{(N-L-1)P_m}{LP_s}x_{s,u}^2\right). \quad (32)$$

Proof See "Appendix 3". □

Theorem 3 *Downlink rate coverage probability of backhaul link, i.e., SBS associated with the MBS is given as*

$$C_b = 2\pi\lambda_m \int_0^\infty x_{m,s}\left[\frac{1}{2} - \frac{1}{\pi}T_2(x)\right]e^{-\pi\lambda_m x_{m,s}^2}dx_{m,s}, \quad (33)$$

where

$$T_2(x) = \int_0^\infty Im[\exp(\vartheta_1(x,\omega) + \vartheta_2(x,\omega) + \vartheta_3(x,\omega))]\frac{d\omega}{\omega}, \quad (34)$$

$$\vartheta_1(x,\omega) = -\pi\lambda_m\left(\frac{\left|1-\frac{2}{\delta}\right| + \frac{2}{\delta}\left|\frac{-2}{\delta}, \frac{j\omega P_m}{x_{m,s}^\delta}\right|}{(j\omega P_m)^{-2/\delta}} - x_{m,s}^2\right), \quad (35)$$

$$\vartheta_2(x,\omega) = -\frac{2\pi\lambda_s P_s j\omega}{\delta-2}x_{m,s}^{2-\delta}{}_2F_1\left[1, 1-\frac{2}{\delta}, 2-\frac{2}{\delta}, \frac{j\omega P_s}{x_{m,s}^\delta}\right], \quad (36)$$

$$\vartheta_3(x,\omega) = -j\omega\left(\frac{P_m}{\tau_b x_{m,s}^\delta} - \alpha P_s\right). \quad (37)$$

Proof See "Appendix 4". □

4.2 Area spectral efficiency (ASE)

ASE performance metric measures spectrum utilization efficiency of a cellular network with variable transmission rate [37, 38]. ASE is defined as maximum data rate per unit bandwidth for a given user over cell coverage area where the user is randomly located [37]. ASE of the proposed model can be calculated as

$$ASE = \lambda_m C_m \log\left(1+\tau_{a,m}\right) + \lambda_s C_s \log\left(1+\min\left\{\tau_{a,s}, \tau_b\right\}\right), \quad (38)$$

where $C_s = C_b \times C_p$ and C_m, C_p, C_b, $\tau_{a,m}$, $\tau_{a,s}$, and τ_b are specified in Sect. 4.1.

5 Numerical results and discussion

This section provides numerical results to investigate the performance of the proposed model. Downlink coverage probability and ASE of a typical user in IBFD mode with respect to different parameters are plotted by utilizing Eqs. (20), (21), (22), and (38). Later on, for getting optimal performance on practical grounds, trade-off between ASE and coverage probability is established. Validity of the derived analytical results is established via Monte Carlo simulation. For simulation purpose, the base station densities are considered as $\lambda_m' = 5$, and $\lambda_s' = 20$. Total number of antennas available at MBS $N = 100$, and $L = 20$ are the total number of supported downlink streams. All the simulation results are obtained with self-interference cancellation value $\alpha = 0$. The rest of the simulation parameter values are stated in Table 1. Unless mentioned, aforementioned parameter values are considered throughout the simulation.

Figures 2 and 3 plot coverage probability against number of antennas and SBS density. As expected downlink coverage probability of MBS is higher than SBS and this is because of huge antenna gain at MBS. The coverage probability of the proposed model enhances on raising the antenna number at MBS. The underlying reason is that antenna gain improves with the increase in number of antennas. Besides, as the number of antennas increases, finer spatial focusing (i.e., sharp beamforming) can be achieved for the desired user. Apart from this, inter-tier interference can also be reduced due to sharp beam formation.

Figure 3 plots the coverage probability versus base station density of small cells. It is observed that by increasing the number of SBSs, the rate coverage probability improves, similar to given in [24]. This is due to decrease in distance between SBS and user with the increase in SBS density. However, coverage becomes constant after certain density limit. This is mainly due to the concordance between inter-tier interference and intra-tier interference in IBFD systems. If more users are offloaded to SBS tier, more backhauling is needed on the same spectrum due to in-band full-duplex strategy which eventually results in large interference to the access links.

Table 1 Basic parameter values for simulation

Parameters	Values
Path loss exponent δ	4
Transmission power for MBS P_m	10 watts
Transmission power for SBS P_s	2 watts
Desired transmission rate R_{th}	1 bps/Hz
Bandwidth allocation factor η	0.5
Large scale fading parameters μ, σ	1 dB, 2 dB
Noise power density N_0	− 100 dBm

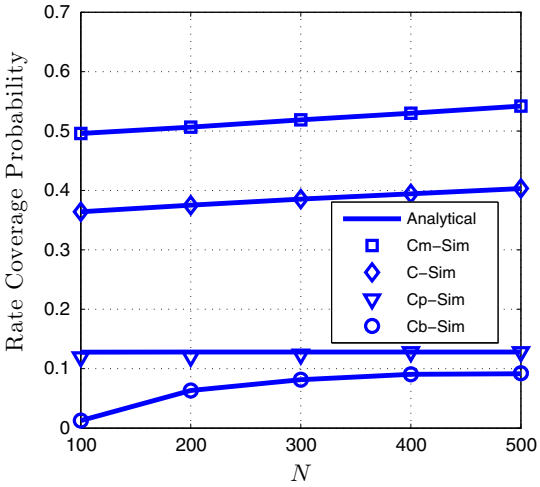

Fig. 2 Rate coverage probability versus number of antennas

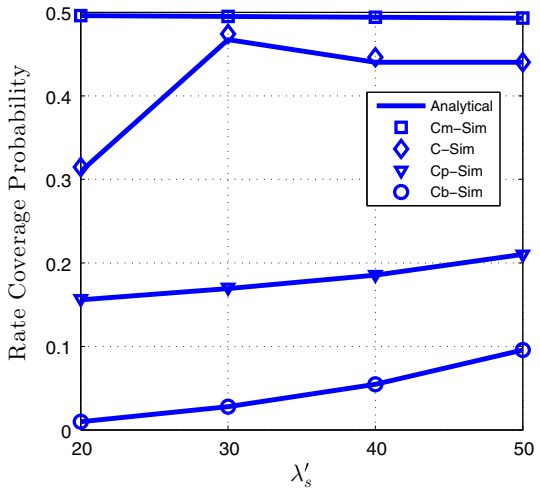

Fig. 3 Rate coverage probability versus SBS density

Hence, coverage probability can further be improved by using more efficient interference mitigation schemes which can be the part of future research work.

Figure 4 depicts the plot of ASE versus SBS density for distinct values of MBS density. It is observed that increase in the SBS and MBS density enhances the ASE of the system which is directly reflected by the ASE presented in (38). The reason of high improvement in ASE with the increase in MBS density is the high antenna gain and sharp beamforming. Hence, massive MIMO at MBS can assist multiple users and can impart backhauling simultaneously with less interference.

Figure 5 exhibits trade-off between ASE and rate coverage probability. ASE and coverage probability are plotted as a function of number of antennas and MBS density. As discussed earlier, the coverage probability improves on raising the antenna number at MBS and this is due to large antenna gain and sharp beamforming. Besides this, from

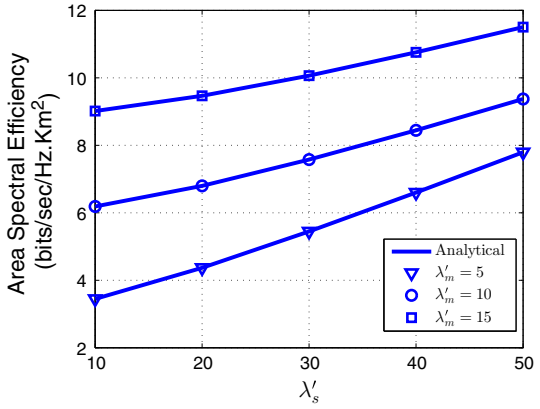

Fig. 4 Area spectral efficiency versus SBS density for different MBS density

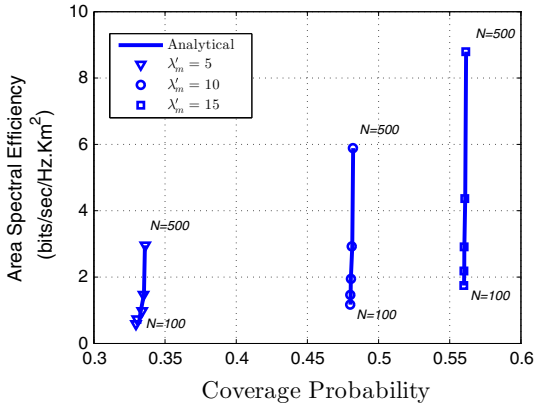

Fig. 5 Trade-off between ASE and rate coverage probability for different MBS density

(38) it can be noticed that ASE is a function of coverage probability and increases with the increase in coverage probability. Hence, this proves the improvement in ASE with the proliferation of antennas. On the other hand, with the increase in MBS density, MBS will provide service to more number of users with considerably higher SINR value henceforth, improves the overall performance with less number of small cell BSs.

Figure 6 shows the trade-off between ASE and coverage probability for different values of η (bandwidth allocation factor). On increasing the value of η, bandwidth required to serve users associated to MBS increases, hence improves the ASE and coverage probability of users associated with MBS only. Whereas, bandwidth (i.e., $(1-\eta)$) allocated for the link that enables transmission from SBS to user and for backhauling (MBS to SBS) decreases. Due to this, interference on both SBS to user link and backhaul link increases and hence, this reduces overall performance of the system.

The effect of path loss on the performance of the massive MIMO enabled heterogeneous network is shown in

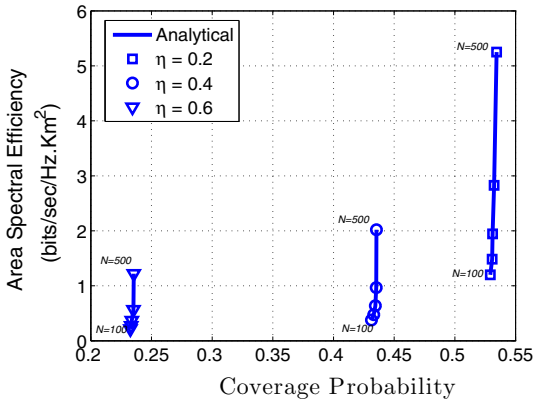

Fig. 6 Trade-off between ASE and rate coverage probability for different values of bandwidth allocation factor

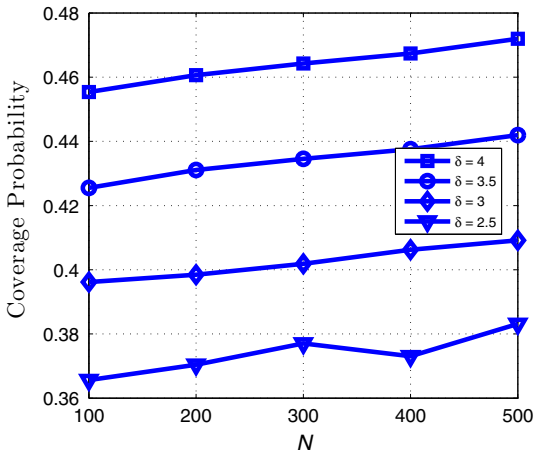

Fig. 7 Rate coverage probability for different path loss exponent (δ)

Fig. 7. Coverage probability of the system improves considerably for higher value of path loss exponent. This is because, large path loss exponent values help to reduce interference between macro cell and small cell. This results in isolation between macro cell and small cell by performing the virtual cell splitting. Henceforth, this helps to achieve dense deployment of IBFD small cells in the network to obtain their mutual benefits.

Coverage probability versus number of antennas for distinct combinations of MBS and SBS transmit powers is shown in Fig. 8. Coverage probability improves with the rise in transmit power at MBS which is mainly due to achieving high SINR for both access link from MBS to user in (11) and backhaul link in (17). This is owing to large received signal strength from the MBS. Whereas on increasing power at SBS, the coverage probability reduces because of the increase in interference at the serving node from the other nearby SBSs.

Finally, in Fig. 9, the performance of the propounded framework is compared with the network model discussed in [6]. Coverage probability of the model provided in [6] is

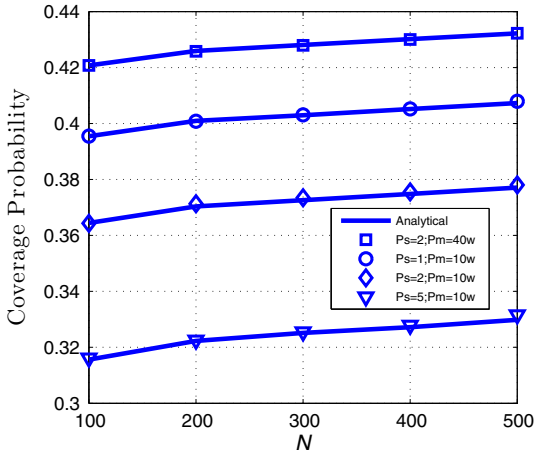

Fig. 8 Rate coverage probability for different combination of SBS and MBS transmit power

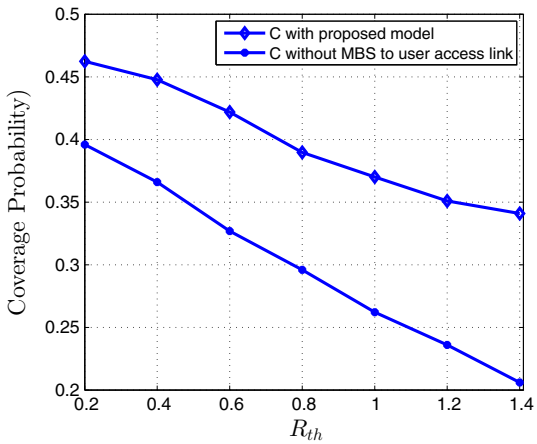

Fig. 9 Rate coverage probability versus R_{th}

plotted by using (22) with $\eta = 0$. From the figure, it can be observed that the proposed model achieves better performance over [6] in terms of coverage probability. It can be noticed that there is an improvement of 42.30% in the coverage performance for rate threshold of $1bps\ /\ Hz$. This is because, when MBS to user link is absent many of the users which are not in the range of SBSs will experience an outage. However, in our framework these users are served by MBS with a higher SINR value due to large antenna gain of massive MIMO. Similarly, ASE for the model given in [6] can also be plotted by considering only the second term on the right-hand side of (38) ($\lambda_s C_s \log\left(1 + \min\left\{\tau_{a,s}, \tau_b\right\}\right)$) with $\eta = 0$, and performance improvement with our model can be noticed.

5.1 Extension to incorporate the effect of imperfect CSI

The work presented above has considered the case of perfect CSI to simplify the analysis for getting some key

insights into system performance. However, in this section, a brief idea is provided to obtain results with imperfect CSI. As large scale fading coefficients mainly depend upon the distance between two communicating nodes and path loss, they can be perfectly estimated due to its property of slow change [39]. On the other hand, MMSE can be performed to estimate the small scale fading coefficients. By the application of MMSE, the estimated small scale fading coefficient can directly be obtained from the standard results in estimation theory [40] and is given as

$$\hat{g} = \sqrt{1-\sigma_e^2}g + \sigma_e \Omega, \tag{39}$$

where $\hat{g}$ and g are the estimated and accurate channel gains. $\Omega \sim CN(0,1)$ and $\sigma_e \in [0,1]$ is the channel estimation error of user. Explicitly, σ_e measures the quality of CSI and $\sigma_e = 0$ indicates the case of perfect CSI and $\sqrt{1-\sigma_e^2}$ represents the correlation coefficient between the estimated and the exact values of channel gain.With this, SINR expressions given in (14) can be modified as $SINR_{a,s} = \frac{P_s \hat{g}_{s,u} \left| X_{s,u} \right|^{-\delta}}{\hat{I}_{m,u_s} + \hat{I}_{s,u_s} + N_0}$, [39]. SINR for other links can be obtained in similar way. After then, coverage probability and ASE expressions can be obtained by following the same derivation steps provided in Sect. 4.

6 Conclusion

This paper has investigated the downlink performance of a two-tier heterogeneous network accounting massive MIMO enabled wireless backhauling at MBS and full-duplex transmission at SBS. Using the concepts of stochastic geometry, tractable and easily computable analytical expressions of rate coverage probability and ASE are derived for IBFD transmission. The closeness between numerical results and simulation results proves the validity of the proposed work. From the numerical results, it is shown that number of antennas and SBS density can be considered as a useful design parameter in the system model to achieve optimal performance. The idea can be outstretched by employing multiple antennas at SBS to serve multiple users and by addressing interference management schemes. From this work, it may be concluded that massive MIMO enabled wireless backhaul and full-duplex transmission are significant technologies for future networks with proper interference management.

Appendix 1: Proof of Lemma 1

Let q denotes the index of the serving tier. Also, the index of the MBS and SBS tier are represented as m and s, respectively. Accordingly, the probability that user is served by MBS is

$$\Pi_m = P[q = m], \tag{40}$$

$$= E_{T_m}[P[P_m{}'(T_m) > P_s{}']], \tag{41}$$

$$\overset{(a)}{=} E_{T_m}\left[P\left[T_s > \left(\frac{LP_s}{(N-L-1)P_m}\right)^{1/\delta} T_m\right]\right], \tag{42}$$

$$\overset{(b)}{=} \int_0^\infty P\left[T_s > \left(\frac{LP_s}{(N-L-1)P_m}\right)^{1/\delta} T_m\right] f_{T_m}(t)dt, \tag{43}$$

where (a) is obtained by substituting (2) and (3) in (40) and (b) can be obtained by averaging $P(\bullet)$ in (41) over the distribution of T_m. Moreover, $P\left[T_s > \left(\frac{LP_s}{(N-L-1)P_m}\right)^{1/\delta} T_m\right]$ and $f_{T_m}(t)$ can be derived by the application of the null probability of a 2-D Poisson process with density λ in an area A is $exp(\lambda A)$. Following this

$$P\left[T_s > \left(\frac{LP_s}{(N-L-1)P_m}\right)^{1/\delta} T_m\right], \tag{44}$$

$$= P[\textit{no BS closer than } \left(\frac{LP_s}{(N-L-1)P_m}\right)^{1/\delta} T_m \textit{ in MBS tier}] \tag{45}$$

$$= \exp\left(-\pi\lambda_s \left(\frac{LP_s}{(N-L-1)P_m}\right)^{1/\delta} t^2\right), \tag{46}$$

and

$$f_{T_m}(t) = 1 - \frac{d}{dt}P[T_m > t], \tag{47}$$

$$= 2\pi\lambda_m t\, e^{-\pi\lambda_m t^2}. \tag{48}$$

Appendix 2: Proof of Theorem 1

Proceeding with (21), downlink rate coverage probability of MBS to user link can be derived as

$$C_m = E_{X_{m,u}} P\left[SINR_{a,m} > \tau_{a,m} \middle| X_{m,u} = x_{m,u}\right], \tag{49}$$

$$C_m = \int_{x_{m,u} > 0} P\left[SINR_{a,m} > \tau_{a,m} \middle| X_{m,u} = x_{m,u}\right] \times f_{X_{m,u}}(x_{m,u})\, dx_{m,u}. \tag{50}$$

After substituting the values of $SINR_{a,m}$ and $f_{X_{m,u}}(x_{m,u})$ from (11) and (6), (50) can be modified as

$$C_m = \frac{2\pi\lambda_m}{\Pi_m} \int\limits_{x_{m,u}>0} F_{I_1}\left[\frac{P_m}{\tau_{a,m}\, x_{m,u}^{\delta}} - N_0\right] x_{m,u} \times e^{\left[-\pi\lambda_m x_{m,u}^2 - \pi\lambda_s\left(\frac{LP_s}{(N-L-1)P_m} x_{m,u}^2\right)\right]} dx_{m,u}, \tag{51}$$

where $F_{I_1}[\bullet]$ is the CDF of the aggregate interference, and Gil-Pelaez theorem is applied to evaluate the aforementioned CDF.

$$F_{I_1}\left[\frac{P_m}{\tau_{a,m}\, x_{m,u}^{\delta}} - N_0\right] = \frac{1}{2} - \frac{1}{\pi} \times \int\limits_0^{\infty} Im\left(L_{I_1}(-j\omega)\, e^{-j\omega\left(\frac{P_m}{\tau_{a,m} x_{m,u}^{\delta}} - N_0\right)}\right) \frac{d\omega}{\omega}, \tag{52}$$

$$= \frac{1}{2} - \frac{1}{\pi} \int\limits_0^{\infty} Im\left(L_{I_{m,u_m}}(-j\omega) L_{I_{s,u_m}}(-j\omega) \times e^{-j\omega\left(\frac{P_m}{\tau_{a,m} x_{m,u}^{\delta}} - N_0\right)}\right) \frac{d\omega}{\omega}, \tag{53}$$

herein $L_{I_{m,u_m}}(s)$ and $L_{I_{s,u_m}}(s)$ are the Laplace transform of the interferences I_{m,u_m} and I_{s,u_m}, respectively and can be derived as follows

$$L_{I_{m,u_m}}(s) = E_{I_{m,u_m}}\left[e^{-sI_{m,u_m}}\right], \tag{54}$$

$$= E\left[s \sum_{i\in\Phi_x/m} P_m \left|X_{i,u}\right|^{-\delta}\right], \tag{55}$$

$$\underline{\underline{(a)}}\; E_{\Phi_x}\left[\prod_{i\in\Phi_x/m} E_g\left\{\exp\left(P_m \left|x_{i,u}\right|^{-\delta}\right)\right\}\right], \tag{56}$$

$$\underline{\underline{(b)}}\; \exp\left(-2\pi\lambda_m \int\limits_{x_{m,u}}^{\infty} \left[1 - \exp\left(sP_m {x_{i,u}}^{-\delta}\right)\right] x_{i,u} dx_{i,u}\right), \tag{57}$$

$$\underline{\underline{(c)}}\; \exp\left[-\pi\lambda_m \left(\frac{\left|1 - \frac{2}{\delta}\right| + \frac{2}{\delta}\left|\frac{-2}{\delta}, \frac{sP_m}{x_{m,u}^{\delta}}\right|}{(sP_m)^{-2/\delta}} - x_{m,u}^2\right)\right], \tag{58}$$

where (a) is due to the independence of interfering links, (b) follows the probability generating functional (PGFL) of PPP, and (c) is achieved by solving the integration.

Thereafter, $L_{I_{s,u_m}}(s)$ can be calculated as

$$L_{I_{s,u_m}}(s) = E_{\Phi_y}\left[\prod_{j\in\Phi_y} E_g\left\{\exp\left(sP_s g_{j,u} \left|X_{j,u}\right|^{-\delta}\right)\right\}\right], \tag{59}$$

by the PGFL of PPP

$$= \exp\left(-2\pi\lambda_s \int\limits_0^{\infty} \left[1 - E_g\left\{\exp\left(sP_s g_{j,u} \left|x_{j,u}\right|^{-\delta}\right)\right\}\right] \times x_{j,u}\, dx_{j,u}\right), \tag{60}$$

$$L_{I_{s,u_m}}(s) = \lim_{x_{s,u}\to 0} L'_{I_{s,u_m}}(s), \tag{61}$$

$$L'_{I_{s,u_m}}(s) = \exp\left(-2\pi\lambda_s \int\limits_{x_{s,u}}^{\infty} \left[1 - E_g\left\{\exp\left(sP_s g_{j,u} \left|x_{j,u}\right|^{-\delta}\right)\right\}\right] \times x_{j,u}\, dx_{j,u}\right), \tag{62}$$

$$= \exp\left(-2\pi\lambda_s \int\limits_{x_{s,u}}^{\infty} \left[1 - \frac{1}{1 + sP_s g_{j,u} {x_{j,u}}^{-\delta}}\right] x_{j,u}\, dx_{j,u}\right), \tag{63}$$

$$= \exp\left(-\frac{2\pi\lambda_s P_s s}{\delta - 2}\, x_{s,u}^{2-\delta}\, {}_2F_1\left[1, 1 - \frac{2}{\delta}, 2 - \frac{2}{\delta}, \frac{sP_s}{x_{s,u}^{\delta}}\right]\right). \tag{64}$$

Now, from (60)

$$L_{I_{s,u_m}}(s) = \lim_{x_{s,u}\to 0} \exp\left(-\frac{2\pi\lambda_s P_s s}{\delta - 2}\, x_{s,u}^{2-\delta}\, {}_2F_1\left[1, 1 - \frac{2}{\delta}, 2 - \frac{2}{\delta}, \frac{sP_s}{x_{s,u}^{\delta}}\right]\right). \tag{65}$$

By using the Kumar's formula

$${}_2F_1[a, b, c, z] = (1 - z)^{-b}\, {}_2F_1\left[c - a, b, c, \frac{z}{z - 1}\right], \tag{66}$$

$$L_{I_{s,u_m}}(s) = \lim_{x_{s,u}\to 0} \exp\left(-\frac{2\pi\lambda_s P_s s}{\delta - 2} \left(x_{s,u}^{\delta} - sP_s\right)^{2-\delta/\delta} {}_2F_1\left[1 - \frac{2}{\delta}, 1 - \frac{2}{\delta}, 2 - \frac{2}{\delta}, \frac{sP_s}{sP_s - x_{s,u}^{\delta}}\right]\right), \tag{67}$$

$$L_{I_{s,u_m}}(s) = \exp\left(\frac{2\pi\lambda_s}{\delta - 2} (-sP_s)^{2/\delta} \left|2 - \frac{2}{\delta}\right| \left|\frac{2}{\delta}\right|\right). \tag{68}$$

Appendix 3: Proof of Theorem 2

Steps for deriving the coverage probability when a user is connected with SBS are as follows

$$C_p = P\left[SINR_{a,s} > \tau_{a,s} \left| X_{s,u} = x_{s,u}\right.\right], \tag{69}$$

$$C_p = \int_0^{\infty} \frac{2\pi\lambda_s}{\Pi_s} P\left[\frac{P_s g_{s,u}\left|X_{s,u}\right|^{-\delta}}{I_{m,u_s}+I_{s,u_s}+N_0} > \tau_{a,s}\right] \times e^{\left[-\pi\lambda_s x_{s,u}^2 - \pi\lambda_m\left(\frac{(N-L-1)P_m}{LP_s} x_{s,u}^2\right)\right]} x_{s,u}\, dx_{s,u}, \tag{70}$$

where

$$P\left[\frac{P_s g_{s,u}\left|X_{s,u}\right|^{-\delta}}{I_{m,u_s}+I_{s,u_s}+N_0} > \tau_{a,s}\right] \tag{71}$$

$$= P\left[g_{s,u} > \frac{\tau_{a,s}\left(I_{m,u_s}+I_{s,u_s}+N_0\right)}{P_s\left|X_{s,u}\right|^{-\delta}}\right], \tag{72}$$

and $P(\bullet)$ is derived below. Since channel is Rayleigh distributed with unit mean, (71) can be simplified as

$$= L_{I_{s,u_s}}(s) L_{I_{m,u_s}}(s) e^{-\frac{\tau_{a,s} x_{s,u}^{\delta} N_0}{P_s}}, \tag{73}$$

where $L_{I_{s,u_s}}(s)$ and $L_{I_{m,u_s}}(s)$ are the Laplace transform of the interferences I_{s,u_s} and I_{m,u_s}, respectively for $s = \frac{\tau_{a,s} x_{s,u}^{\delta}}{P_s}$. These can be calculated with the same procedure which is explained in Theorem 1 and are given as follows

$$L_{I_{m,u_s}}(s) = E_{\Phi_x}\left[\prod_{i\in\Phi_x} \exp\left(-sP_m x_{i,u}^{-\delta}\right)\right], \tag{74}$$

$$= \exp\left(2\pi\lambda_m \int_0^{\infty} \left(1 - \exp\left[-sP_m x_{i,u}^{-\delta}\right]\right) x_{i,u}\, dx_{i,u}\right), \tag{75}$$

$$= \exp\left(-\pi\lambda_m (sP_m)^{2/\delta} \left|1 - \frac{2}{\delta}\right)\right), \tag{76}$$

$$L_{I_{s,u_s}}(s) = E_{\Phi_y}\left[\prod_{j\in\Phi_{y/s}} \exp\left(-sP_s g_{j,u} x_{j,u}^{-\delta}\right)\right], \tag{77}$$

$$= \exp\left(-2\pi\lambda_s \int_{x_{s,u}}^{\infty} \left(1 - \frac{1}{1+sP_s g_{j,u} x_{j,u}^{-\delta}}\right) x_{j,u}\, dx_{j,u}\right), \tag{78}$$

$$= \exp\left(-\frac{2\pi\lambda_s P_s s}{\delta-2} x_{s,u}^{2-\delta}\, {}_2F_1\left[1, 1-\frac{2}{\delta}, 2-\frac{2}{\delta}, \frac{sP_s}{x_{s,u}^{\delta}}\right]\right). \tag{79}$$

Appendix 4: Proof of Theorem 3

Coverage probability of backhaul link (i.e., SBS associated with the MBS) can be derived analogous to the proof of Theorem 1. Moreover, key steps therein are mentioned below.

$$C_b = P\left[SINR_b > \tau_b \left| X_{m,s} = x_{m,s}\right.\right], \tag{80}$$

$$C_b = 2\pi\lambda_m \int_{x_{m,s}>0} F_{I_2}\left[\frac{P_m}{\tau_b x_{m,s}^{\delta}} - \alpha P_s\right] x_{m,s} \times e^{-\pi\lambda_m x_{m,s}^2}\, dx_{m,s}, \tag{81}$$

where $F_{I_2}(\bullet)$ is the CDF of the aggregate interference, and Gil-Pelaez theorem is applied to evaluate the aforementioned CDF.

$$F_{I_2}\left[\frac{P_m}{\tau_b x_{m,s}^{\delta}} - \alpha P_s\right] = \frac{1}{2} - \frac{1}{\pi} \times \int_0^{\infty} Im\left(L_{I_2}(-j\omega)\, e^{-j\omega\left(\frac{P_m}{\tau_b x_{m,s}^{\delta}} - \alpha P_s\right)}\right) \frac{d\omega}{\omega}, \tag{82}$$

$$F_{I_1}\left[\frac{P_m}{\tau_b x_{m,s}^{\delta}} - \alpha P_s\right] = \frac{1}{2} - \frac{1}{\pi} \times \int_0^{\infty} Im\left(L_{I_{m,s}}(-j\omega) L_{I_{s,s}}(-j\omega)\, e^{-j\omega\left(\frac{P_m}{\tau_b x_{m,s}^{\delta}} - \alpha P_s\right)}\right) \frac{d\omega}{\omega}, \tag{83}$$

where $L_{I_{m,s}}(s)$ and $L_{I_{s,s}}(s)$ are the Laplace transform of the interferences $I_{m,s}$ and $I_{s,s}$, respectively and can be evaluated as

$$L_{I_{m,s}}(s) = E_{I_{m,s}}\left[e^{-sI_{m,s}}\right], \tag{84}$$

$$= E\left[s \sum_{i\in\Phi_x/m} P_m \left|X_{i,s}\right|^{-\delta}\right], \tag{85}$$

$$= \exp\left[-\pi\lambda_m \left(\frac{\left|1 - \frac{2}{\delta}\right| + \frac{2}{\delta}\left|\frac{-2}{\delta}, \frac{sP_m}{x_{m,s}^{\delta}}\right|}{(sP_m)^{-2/\delta}} - x_{m,s}^2\right)\right], \tag{86}$$

$$L_{s,s}(s) = E_{I_{s,s}}\left[e^{-sI_{s,s}}\right], \tag{87}$$

$$= E\left[s \sum_{j\in\Phi_y/s} P_s\, g_{j,s} \left|X_{j,s}\right|^{-\delta}\right], \tag{88}$$

$$= \exp\left(-\frac{2\pi\lambda_s P_s s}{\delta-2} x_{m,s}^{2-\delta}\, {}_2F_1\left[1, 1-\frac{2}{\delta}, 2-\frac{2}{\delta}, \frac{sP_s}{x_{m,s}^{\delta}}\right]\right). \tag{89}$$

References

1. Cisco. (2018). *Cisco visual networking index: Forecast and trends*. https://www.cisco.com/c/en/us/solutions/collateral/service-provider/visual-networking-index-vni/white-paper-c11-741490.html. Accessed Mar 2018.

2. Hwang, I., Song, B., & Soliman, S. S. (2013). A holistic view on hyper-dense heterogeneous and small cell networks. *IEEE Communications Magazine*, *51*(6), 20–27. https://doi.org/10.1109/MCOM.2013.6525591.
3. Kazi, B. U., & Wainer, G. A. (2019). Next generation wireless cellular networks: Ultra-dense multi-tier and multi-cell cooperation perspective. *Wireless Networks*, *25*(4), 2041–2064. https://doi.org/10.1007/s11276-018-1796-y.
4. Kamel, M., Hamouda, W., & Youssef, A. (2016). Ultra-dense networks: A survey. *IEEE Communications Surveys Tutorials*, *18*(4), 2522–2545. https://doi.org/10.1109/COMST.2016.2571730.
5. Kela, P., Costa, M., Turkka, J., Leppanen, K., & Jantti, R. (2016). Flexible backhauling with massive mimo for ultra-dense networks. *IEEE Access*, *4*, 9625–9634. https://doi.org/10.1109/ACCESS.2016.2634039.
6. Tabassum, H., Sakr, A. H., & Hossain, E. (2016). Analysis of massive mimo-enabled downlink wireless backhauling for full-duplex small cells. *IEEE Transactions on Communications*, *64*(6), 2354–2369. https://doi.org/10.1109/TCOMM.2016.2555908.
7. Yang, H. H., Geraci, G., & Quek, T. Q. S. (2016). Energy-efficient design of mimo heterogeneous networks with wireless backhaul. *IEEE Transactions on Wireless Communications*, *15*(7), 4914–4927. https://doi.org/10.1109/TWC.2016.2549529.
8. Larsson, E. G., Edfors, O., Tufvesson, F., & Marzetta, T. L. (2014). Massive mimo for next generation wireless systems. *IEEE Communications Magazine*, *52*(2), 186–195. https://doi.org/10.1109/MCOM.2014.6736761.
9. Rajoria, S., Trivedi, A., & Godfrey, W. W. (2018). A comprehensive survey: Small cell meets massive mimo. *Physical Communication*, *26*, 40–49. https://doi.org/10.1016/j.phycom.2017.11.004.
10. Duarte, M., Sabharwal, A., Aggarwal, V., Jana, R., Ramakrishnan, K. K., Rice, C. W., et al. (2014). Design and characterization of a full-duplex multiantenna system for wifi networks. *IEEE Transactions on Vehicular Technology*, *63*(3), 1160–1177. https://doi.org/10.1109/TVT.2013.2284712.
11. Choi, J. I., Jain, M., Srinivasan, K., Levis, P., & Katti, S. (2010). Achieving single channel, full duplex wireless communication. In *Proceedings of the sixteenth annual international conference on Mobile computing and networking (MobiCom '10)* (pp 1–12). New York, NY: ACM. https://doi.org/10.1145/1859995.1859997.
12. Chen, L., Yu, F. R., Ji, H., Rong, B., & Leung, V. C. M. (2018). Power allocation in small cell networks with full-duplex self-backhauls and massive mimo. *Wireless Networks*, *24*(4), 1083–1098. https://doi.org/10.1007/s11276-016-1381-1.
13. Li, B., Zhu, D., & Liang, P. (2015). Small cell in-band wireless backhaul in massive mimo systems: A cooperation of next-generation techniques. *IEEE Transactions on Wireless Communications*, *14*(12), 7057–7069. https://doi.org/10.1109/TWC.2015.2464299.
14. Shojaeifard, A., Wong, K. K., Di Renzo, M., Zheng, G., Hamdi, K. A., & Tang, J. (2017). Massive mimo-enabled full-duplex cellular networks. *IEEE Transactions on Communications*, *65*(11), 4734–4750. https://doi.org/10.1109/TCOMM.2017.2731768.
15. Dhillon, H. S., Ganti, R. K., & Andrews, J. G. (2011). A tractable framework for coverage and outage in heterogeneous cellular networks. In: *Proceedings of 2011 Information Theory and Applications Workshop* (pp. 1–6). https://doi.org/10.1109/ITA.2011.5743604.
16. Jiang, Y., Zou, Y., Guo, H., Tsiftsis, T. A., Bhatnagar, M. R., de Lamare, R. C., et al. (2019). Joint power and bandwidth allocation for energy-efficient heterogeneous cellular networks. *IEEE Transactions on Communications*, *67*(9), 6168–6178. https://doi.org/10.1109/TCOMM.2019.2921022.
17. Xie, Y., Li, B., Zuo, X., Yan, Z., & Yang, M. (2018). Performance analysis for 5g beamforming heterogeneous networks. *Wireless Networks*,. https://doi.org/10.1007/s11276-018-1846-5.
18. He, A., Wang, L., Chen, Y., Elkashlan, M., & Wong, K. (2015). Massive MIMO in k-tier heterogeneous cellular networks: Coverage and rate. In: *2015 IEEE Global Communications Conference (GLOBECOM)* (pp. 1–6). https://doi.org/10.1109/GLOCOM.2015.7417732.
19. He, A., Wang, L., Elkashlan, M., Chen, Y., & Wong, K. K. (2015). Spectrum and energy efficiency in massive mimo enabled hetnets: A stochastic geometry approach. *IEEE Communications Letters*, *19*(12), 2294–2297. https://doi.org/10.1109/LCOMM.2015.2493060.
20. Li, C., Zhang, J., Andrews, J. G., & Letaief, K. B. (2016). Success probability and area spectral efficiency in multiuser mimo hetnets. *IEEE Transactions on Communications*, *64*(4), 1544–1556. https://doi.org/10.1109/TCOMM.2016.2531719.
21. Xie, H., Gao, F., Zhang, S., & Jin, S. (2017). A unified transmission strategy for tdd/fdd massive mimo systems with spatial basis expansion model. *IEEE Transactions on Vehicular Technology*, *66*(4), 3170–3184. https://doi.org/10.1109/TVT.2016.2594706.
22. Ma, J., Zhang, S., Li, H., Gao, F., & Jin, S. (2019). Sparse bayesian learning for the time-varying massive mimo channels: Acquisition and tracking. *IEEE Transactions on Communications*, *67*(3), 1925–1938. https://doi.org/10.1109/TCOMM.2018.2855197.
23. Ma, J., Zhang, S., Li, H., Zhao, N., & Leung, V. C. M. (2018). Interference-alignment and soft-space-reuse based cooperative transmission for multi-cell massive mimo networks. *IEEE Transactions on Wireless Communications*, *17*(3), 1907–1922. https://doi.org/10.1109/TWC.2017.2786722.
24. Akbar, S., Deng, Y., Nallanathan, A., Elkashlan, M., & Karagiannidis, G. K. (2017). Massive multiuser mimo in heterogeneous cellular networks with full duplex small cells. *IEEE Transactions on Communications*, *65*(11), 4704–4719. https://doi.org/10.1109/TCOMM.2017.2728536.
25. Sharma, A., Ganti, R. K., & Milleth, J. K. (2017). Joint backhaul-access analysis of full duplex self-backhauling heterogeneous networks. *IEEE Transactions on Wireless Communications*, *16*(3), 1727–1740. https://doi.org/10.1109/TWC.2017.2653108.
26. Zhang, Z., Wang, X., Long, K., Vasilakos, A. V., & Hanzo, L. (2015). Large-scale mimo-based wireless backhaul in 5g networks. *IEEE Wireless Communications*, *22*(5), 58–66. https://doi.org/10.1109/MWC.2015.7306538.
27. Chen, D. C., Quek, T. Q. S., & Kountouris, M. (2015). Backhauling in heterogeneous cellular networks: Modeling and tradeoffs. *IEEE Transactions on Wireless Communications*, *14*(6), 3194–3206. https://doi.org/10.1109/TWC.2015.2403321.
28. Chen, L., Yu, F. R., Ji, H., Rong, B., Li, X., & Leung, V. C. M. (2016). Green full-duplex self-backhaul and energy harvesting small cell networks with massive mimo. *IEEE Journal on Selected Areas in Communications*, *34*(12), 3709–3724. https://doi.org/10.1109/JSAC.2016.2611846.
29. Liu, Y., Lu, L., Li, G. Y., Cui, Q., & Han, W. (2016). Joint user association and spectrum allocation for small cell networks with wireless backhauls. *IEEE Wireless Communications Letters*, *5*(5), 496–499. https://doi.org/10.1109/LWC.2016.2593465.
30. Wang, N., Hossain, E., & Bhargava, V. K. (2016). Joint downlink cell association and bandwidth allocation for wireless backhauling in two-tier hetnets with large-scale antenna arrays. *IEEE Transactions on Wireless Communications*, *15*(5), 3251–3268. https://doi.org/10.1109/TWC.2016.2519401.

31. Andrews, J. G., Gupta, A. K., & Dhillon, H. S. (2016). A primer on cellular network analysis using stochastic geometry. *CoRR*. arXiv:1604.03183.
32. Benmimoune, M., Driouch, E., Ajib, W., & Massicotte, D. (2017). Novel transmit antenna selection strategy for massive mimo downlink channel. *Wireless Networks*, *23*(8), 2473–2484. https://doi.org/10.1007/s11276-016-1297-9.
33. Hosseini, K., Yu, W., & Adve, R. S. (2014). Large-scale mimo versus network mimo for multicell interference mitigation. *IEEE Journal of Selected Topics in Signal Processing*, *8*(5), 930–941. https://doi.org/10.1109/JSTSP.2014.2327594.
34. Jo, H. S., Sang, Y. J., Xia, P., & Andrews, J. G. (2012). Heterogeneous cellular networks with flexible cell association: A comprehensive downlink sinr analysis. *IEEE Transactions on Wireless Communications*, *11*(10), 3484–3495. https://doi.org/10.1109/TWC.2012.081612.111361.
35. Thilina, K. M., Tabassum, H., Hossain, E., & Kim, D. I. (2015). Medium access control design for full duplex wireless systems: challenges and approaches. *IEEE Communications Magazine*, *53*(5), 112–120. https://doi.org/10.1109/MCOM.2015.7105649.
36. Masmoudi, A., & Le-Ngoc, T. (2017). *Full-duplex wireless communications systems*. Berlin: Springer. https://doi.org/10.1007/978-3-319-57690-9.
37. Alouini, M., & Goldsmith, A. J. (1999). Area spectral efficiency of cellular mobile radio systems. *IEEE Transactions on Vehicular Technology*, *48*(4), 1047–1066. https://doi.org/10.1109/25.775355.
38. Xin, Y., Wang, D., Li, J., Zhu, H., Wang, J., & You, X. (2016). Area spectral efficiency and area energy efficiency of massive mimo cellular systems. *IEEE Transactions on Vehicular Technology*, *65*(5), 3243–3254. https://doi.org/10.1109/TVT.2015.2436896.
39. Jose, J., Ashikhmin, A., Marzetta, T. L., & Vishwanath, S. (2011). Pilot contamination and precoding in multi-cell tdd systems. *IEEE Transactions on Wireless Communications*, *10*(8), 2640–2651. https://doi.org/10.1109/TWC.2011.060711.101155.
40. Wang, C., Au, E. K. S., Murch, R. D., & Lau, V. K. N. (2006). Closed-form outage probability and ber of mimo zero-forcing receiver in the presence of imperfect csi. In *2006 IEEE 7th workshop on signal processing advances in wireless communications* (pp. 1–5). https://doi.org/10.1109/SPAWC.2006.346359.

Shweta Rajoria received her B.E. in Electronics and Communication Engineering from SRCEM Gwalior, India. She did her M.E. in Electronics and Telecommunication Engineering from SGSITS, Indore, India. Currently, she is pursuing her Ph.D. from Department of Information and Communication Technology at ABV-Indian Institute of Information Technology and Management, Gwalior, India. Her areas of interest are Massive MIMO, small cells, stochastic geometry, and Optimization Techniques.

Aditya Trivedi is a Professor in the ICT Department of ABV-Indian Institute of Information Technology and Management, Gwalior, India. He received his bachelor degree (with distinction) in Electronics Engineering. from the Jiwaji University. He did his M.Tech. (Communication Systems) from Indian Institute of Technology (IIT), Kanpur. He obtained his doctorate (Ph.D.) from IIT Roorkee in the area of Wireless Communication Engineering. His teaching and research interest include Digital communication, CDMA systems, Signal processing, and Networking. He is a fellow of the Institution of Electronics and Telecommunication Engineers (IETE) and a senior member of Institution of Electrical and Electronics Engineers (IEEE), USA. Dr. Trivedi has guided many Ph.D. theses. He has guided more than hundreds of M.Tech. theses. Dr. Trivedi is a reviewer of reputed IEEE and Springer journals. He has published more than 100 papers in various prestigious International/National journals and conferences. In 2007, he was given the IETE's K.S. Krishnan Memorial Award for best system oriented paper. He has delivered talks in various places related to wireless communication and networking.

W. Wilfred Godfrey is a Assistant Professor in the ICT Department of ABV-Indian Institute of Information Technology and Management, Gwalior, India. He received his Bachelors in Computer Science and Engineering from Manonmanium Sundaranar University (Tamil Nadu), Masters in Computer Science and Engineering from Govternment College of Technology Coimbatore, Ph.D. in Computer Science and Engineering from Indian Institute of Technology Guwahati. He has also worked in Samsung as a Lead Engineer. His teaching and research interest include Artificial Intelligence, Robotics and Machine Learning. He has two Indian patents.